Development of a Novel Wireless Multi-Channel Stethograph System for Monitoring Cardiovascular and Cardiopulmonary Diseases

XINGZHE ZHANG , (Member, IEEE), **DINESH MADDIPATLA** , (Member, IEEE),
BINU B. NARAKATHU , (Member, IEEE), **BRADLEY J. BAZUIN** , (Member, IEEE),
AND MASSOOD Z. ATASHBAR , (Senior Member, IEEE)
Electrical Engineering Department, Western Michigan University, Kalamazoo, MI 49008, USA

Corresponding author: Xingzhe Zhang (xingzhe.zhang@wmich.edu)

ABSTRACT A multi-channel stethograph system was designed and developed as an electronic auscultation system for graphic recording of heart, lung, and trachea (HLT) sounds non-invasively through a set of 16 acoustic sensors. The multi-channel stethograph system was fabricated by placing 16 microphone based acoustic sensor in a CNC machined Delrin®housing cases that are covered using diaphragms. Among the 16 acoustic sensors, 14 were positioned in a memory foam pad, and two were placed directly on the heart and trachea to acquire sounds simultaneously from the lungs, heart, and trachea. The sounds acquired from the 16 acoustic sensors were processed through a custom designed and fabricated 16-channel PCB for signal conditioning. A National Instruments (NI) 9205 data acquisition device (DAQ) along with a NI 9191 wireless chassis was used to acquire and wirelessly transmit the data from the 16-channel PCB to a Wi-Fi enabled device such as a PC/tablet. A custom LabVIEW program was developed on a Wi-Fi enabled PC/tablet to record the data from the DAQ. In addition, a MATLAB program was developed to convert the recorded data from the acoustic sensors into 16 audio files (for audio playback) and plot the waveforms in time and frequency domain as well as spectrogram for visual examination of any abnormal patterns in inhalation and exhalation. This provides critical information on the presence of crackles, rhonchi and wheeze sounds as well as abnormal heartbeat and respiration rate which helps in analyzing the condition of heart and lungs. The graphically displayed HLT sounds will help physicians in the clinical diagnosis and monitoring of lung and heart disorders, particularly chronic obstructive pulmonary disease (COPD), asthma, pneumonia, and congestive heart failure by providing objective evidence.

INDEX TERMS Acoustic sensor, heart, lung and trachea (HLT) sounds, multi-channel wireless stethograph system, non-invasive, signal conditioning board.

I. INTRODUCTION

Cardiovascular and cardiopulmonary diseases (CCD) such as pneumonia, COPD (chronic obstructive pulmonary disease), and CHF (congestive heart failure) is prevalent in the US [1]–[3]. According to American Thoracic Society, pneumonia is considered the world's leading cause of death (880,000 deaths were estimated in 2016) among children under the age of 5 [1]. In the United States alone, more than 55,000 die from this disease, with about 1 million adults

The associate editor coordinating the review of this manuscript and approving it for publication was Chunsheng Zhu .

seeking hospital care each year. Chronic lower respiratory disease, primarily COPD, is the fourth leading cause of death in the United States with 140,000 death each year (1 death every 4 minutes!) [2]. Almost 15 million Americans were diagnosed with COPD. In addition to Pneumonia and COPD, CHF is also a serious problem with ≈550,000 new cases being reported in the U.S. each year. Currently, 5 million people are diagnosed with CHF in the United States, and 287,000 deaths were reported to be linked to heart failures in a year [3].

CCDs are mainly diagnosed by chest X-ray, CT scan, and blood test [4]. However, some of these methods are not

considered safe for multiple/repetitive tests (do not support continuous diagnosing of patients) due to the radiation exposure. Some are invasive and are associated with high costs. Typically, when breathing, a patient with pneumonia exhibits crackles sound, and abnormal respiratory rate, a patient with COPD has rhonchi and wheeze sounds. CHF causes crackle sound and abnormal heart rate in the patient [5]. To diagnose the CCD diseases efficiently in a simple way is to observe and identify these adventitious sounds, heart and respiratory rates in the heart, lung, and trachea (HLT) sounds. Stethoscopes are validated as a non-invasive and low-cost tool to perform the preliminary diagnosis on CCD [6], [7]. Stethoscopes are often considered as a symbol of healthcare professionals and have been used since 1816 to obtain acoustic information from the chest, that is helpful in the diagnosis of pulmonary conditions [8]–[12]. In recent years, advancements in electronics and computerized methods have provided the potential to obtain this information more objectively with greater precision which in turn may aid in diagnosis and monitoring of various CCD more accurately and efficiently.

In the past, the heart and lung sounds were detected by placing the ear to the chest. However, with the invention of the stethoscope by Laennec [11], several categories of HLT sounds could be easily detected and classified. Laennec's systematic and thorough clinical pathologic correlation of these sounds was a remarkable achievement and revolutionized the practice of medicine by "altering both the physician's perception of disease and their relation to the patient" [12]. In particular, the stethoscope drew the physician into the private world in which signs (abnormalities in the HLT sounds) were directly communicated to the physician from the patient's body [12]. Nevertheless, clinicians regularly listen to HLT sounds especially lung sound using a stethoscope and this process is subject to a variety of limitations. These include observer variability (human ear is not sensitive to the low frequency band) [8], inadequate understanding of the basic mechanisms of production of the sounds, and the lack of adequate studies of clinical and physiologic correlations of the sounds themselves [12].

To address these problems, many researchers are focusing on developing the computerized lung and heart sound recording systems that can aid in monitoring of various CCD [13]–[20]. For example, E. Messner *et al.*, developed a robust multichannel lung sound recording device by using a commercially available pre-amplifier device "SM Pro Audio EP84 8-channel microphone" with the integrated ADAT interface that is commonly used for computer audio systems, stand-alone hard disk recorders, analog or digital workstations [15]. This pre-amplification device does not facilitate wireless data communication/transmission and provides basic per channel manual control over signal to noise ratio (SNR) or gain of the input signal, thus limiting the signal processing options for improving the quality of the acquired lung sounds [15]. Similarly, S. G. Wong has developed a multi-channel computerized heart sound recording apparatus

that uses a commercially available signal conditioning device (Maxim's MAX9812HEXT+T) which is a fixed-gain microphone amplifier with no control over the gain [14]. The stethoscopes used in these recording devices suffer from cross talk problems due to the lack of isolation circuit in the signal conditioning board and electromagnetic interference (EMI) shielding. G. Karacocuk *et al.* developed a wireless detection system using two separate MPU-9250 PCBs, which were connected via Bluetooth. However, the system did not cover the entire area of the lungs and, therefore, was not capable of recording all the sounds [20]. Further, even though the communication was wireless, the Bluetooth connections suffer from narrow bandwidth, faster signal attenuation, and low transmission distance [20].

Most of the CCD diseases have abnormalities in the heart (rapid heartbeat rate), lung (crackles, rhonchi and wheeze sounds), as well as respiratory systems (rapid respiration rate), and the symptoms can only be identified precisely and efficiently by recording the HLT sounds simultaneously [21]–[25]. In addition, multiple sensors are required to cover the maximum area of the lungs for identifying the exact location of an abnormal sound or event such as mother crackle in Pneumonia and CHF or mother wheeze in COPD and Asthma [26]–[29]. However, there are no devices available currently that can detect the HLT sounds simultaneously and covers the maximum area of the lungs. The commercially available stethoscopes have a single channel with one acoustic sensor for recording the sound and do not have the capability of multi-location measurement simultaneously which is difficult for doctors/physicians to find out the original location of the disease with these devices [6]. Researchers have been focusing on the development of different robust sound recording systems with multi-channel acoustic sensors such as 4 channel and 8 channel that can aid in monitoring various cardiopulmonary diseases [14]–[16], [18]–[20]. However, the accuracy, reliability, and function of those preliminary (initial) systems are still in progress and currently not reaching the standards of commercialization. To overcome these limitations, a computerized multi-channel HLT sound recording system is required and this has led to the research on the development of a robust computerized wireless system to record HLT sounds non-invasively for diagnosing various CCD.

In this work, a multi-channel stethograph system with a custom-built signal conditioning unit and Wi-Fi communication capability was developed for more advanced diagnosis, and monitoring of HLT sounds simultaneously and non-invasively with high precision. The wireless data recording capability enables high portability and provides real time monitoring of data remotely and significantly benefit developing and under developed countries where the patients are located in a hard-to-reach areas where a physician or doctor may not be available. The fabrication details and the simultaneous detection capability of the multi-channel stethograph system is demonstrated.
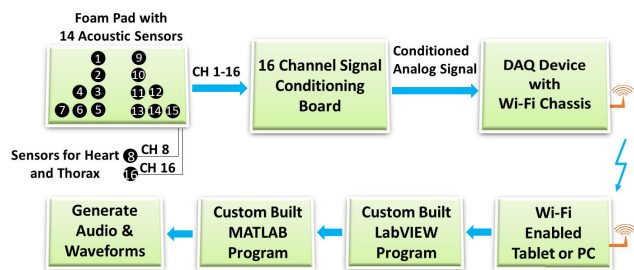
FIGURE 1. Schematic of the multi-channel stethograph system.

TABLE 1. The specifications of the multi-channel stethograph system.

Specification of the Stethograph System	
Supply Voltage	9V
Sampling Rate	8,000 Hz
Operating Frequency	50 ~ 1,600 Hz
Output Amplitude	0.1 V_{pk-pk} to 10 V_{pk-pk}

II. EXPERIMENTAL

A. MATERIALS AND COMPONENTS

A 1'' thick high-density memory foam pad was purchased from Foam N' More Inc., Detroit, MI. Microphones (CMC-5044PF-A CUI) from Mouser Electronics were used for the stethoscopes fabrication. Black Delrin® acetal resin rod from McMASTER-CARR® was used for fabricating the microphone cases. Littmann L40022 diaphragm was purchased from 3M Co., USA. Custom PCB was fabricated at Safari Circuits Inc, USA. A shielded 4-conductor 32 AWG cable (30-00218), 44 position D-sub connector (1757823-9), 25 position two-piece backshell (970-025-030R121), insertion and extraction tool (91067-1), hand crimper tool (PA1460), and 44 position D-Sub cable assembly (CS-DSDHD44MF0-002.5) were used to connect the wires from microphone to PCB and were purchased from DigiKey, USA. 37 position D-Sub cable assembly (2302191) from DigiKey was used to connect the PCB to DAQ. Data acquisition system (NI 9205) and wireless chassis (NI 9191) was purchased from National Instruments. Devices.

B. DEVELOPMENT OF MULTI-CHANNEL STETHOGRAPH SYSTEM

The multi-channel stethograph system consists of a high-density memory foam pad embedded with acoustic sensors, a custom designed and fabricated 16-channel signal conditioning board, data acquisition device with Wi-Fi chassis, and a Wi-Fi enabled device such as PC or tablet with LabVIEW program. The schematic of the system is shown in Fig. 1. In brief, the HLT audio will be acquired from the 16 acoustic sensors and then filtered and amplified using a custom-built signal conditioning board. Following this, the amplified audio signals will be wirelessly transmitted using a National Instruments (NI) 9205 data acquisition device (DAQ) along with a NI 9191 wireless chassis to a Wi-Fi enabled device (PC/Tablet). A custom-built LabVIEW program will be used to real-time plotting of the sounds waveform and recording the data. A MATLAB program will be used to convert the recorded data into 16 audio files and further analysis the data especially heartbeat and respiration rate detection. The specifications of the multi-channel stethograph system shows in Table 1.

1) FABRICATION OF CUSTOM DESIGNED ACOUSTIC SENSOR

Initially the microphones were soldered to cables. A CNC machined cylindrical shaped Delrin® material with height 0.5'' and radius of ∼0.9'' which matches the size of 3M Littmann diaphragm was used as casings to hold the condenser sensor. Microphones were embedded in the Delrin® casings by applying water proof and airtight transparent premium silicone glue on the soldered end of the microphone and by attaching an O-ring washer (5 mm ID, 8 mm OD, 1.5 mm cross section) to the other end of the microphone. The O-ring washer avoids the flow of glue from one end of the casing to other end and holds the microphone. Once the glue is dried/cured (approximately 3 hours), the casings were covered with the Littmann diaphragm. The fabricated acoustic sensors are shown in Fig. 2.

2) MEMORY FOAM PAD ASSEMBLY WITH ACOUSTIC SENSORS

A high-density memory foam pad of 5.3 lb/ft^3 with indentation force deflection (IFD) of 9-10 lbs/50sq.inch was chosen since it provides better compression rates with longer life compared to medium and low-density memory foams. The foam pad assembly consists of top and bottom foam pad layers as shown in Fig. 2(e). 40 mm holes were punched out in the top memory foam pad layer and the acoustic sensors were embedded into the holes. The acoustic sensors were one each for trachea and heart location, to record the HLT audio efficiently and effectively [30], [31]. Then the bottom memory foam pad layer was attached to the backside of top foam layer with the help of a spray adhesive from Loctite®. The photograph of the foam pad with acoustic sensors is shown in Fig. 2(f). The foam pad provides relatively better contact with patient's chest wall as well as comfort to the patient by conforming to the patient's body contour when lying/leaning on the pad and provides acoustic isolation between the sensors.

Among the 16 acoustic sensors, 14 were positioned in the memory foam pad and 2 were placed directly on the heart and trachea to acquire sounds simultaneously from the lungs, heart and trachea. 14 sensors can cover the maximum area of the lungs and record sounds at different locations of lungs simultaneously (Fig. S1, Table SI). With multi-channel sensors, mother adventitious sound and its location can be
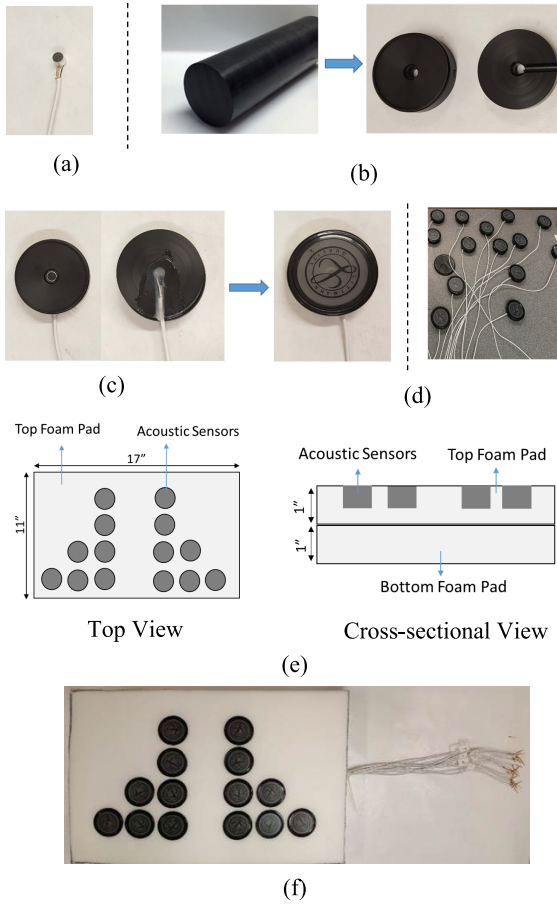
(a)

(b)

(c)

(d)

(e)

(f)

FIGURE 2. (a) Microphone soldered to cable, (b) CNC machined Delrin® casing, (c) Delrin® casing with microphone and diaphragm and (d) multiple acoustic sensors. (e) schematic of the foam pad with acoustic sensors, (f) photograph of the foam pad with acoustic sensors.

determined based on the amplitude of all adventitious sounds in the audios at time domain. The concept of an adventitious sound (crackle, rhonchi and wheeze) family was first introduced and validated by Vyshedskiy *et al.* [7]. The origin location of adventitious sound with highest sound amplitude is called the mother adventitious sound, and the corresponding deflections at other locations are called daughter adventitious sounds. However, without multi-channel sensors, it is difficult and time consuming to accurately measure the sound level in different locations using single stethoscope since the sound level may vary in each breath cycle.

3) SIGNAL CONDITIONING UNIT

Even though the acoustic sensors are meant to detect the sounds from heart (50-200 Hz), lung (80-1600 Hz) and trachea (100 to 1500 Hz), they are also easily prone to external noise such as body noises, ambient/background noises as well as cable noises. The electrical signals generated by the acoustic sensors are very small voltages (<100 mV) and cannot be used directly for further analysis [32]–[34]. To address these issues, a signal conditioning circuit was required to filter and reduce the noise level in the electrical signal and

amplify it for further analysis, such as analog-to-digital (A/D) conversion and signal processing. The signal conditioning circuits implemented in the literature were very simple and did not provide the desired filtering and gain characteristics [14]–[16], [18]–[20]. In addition, these circuits affect the performance of the acoustic sensors due to the absence of any electrical DC isolation or sensor line isolator ICs.

The schematic of the single channel of the custom-designed signal conditioning circuit is shown in Fig. 3(a). The signal conditioning circuit was designed with a gain of 34 and operating frequency ranging from 50 Hz to 1600 Hz. Various components such as capacitors, resistors, op-amp chip, optocoupler (isolator) chips were used for building cascaded signal processing circuits consisting of filters, isolator and amplification. In addition, two power supply circuit designs (power circuit_1 and power circuit_2) were used for generating specific voltages to power the signal conditioning circuit for Section 1 and Section 2, respectively.

a: CUT-OFF FREQUENCY AND AMPLIFICATION GAIN CALCULATION

The designed signal conditioning circuit is divided into 6 stages with each stage performing a particular function. Multiple filtering stages were employed to increase the order of the filter (to attenuate the noise in the input signal). Stage 1 is a first order high pass filter powered by power circuit_1 and it includes a passive high pass filter with cut-off frequency of 2.3 Hz (for blocking the DC) (Eq. (1)) and a non-inverting amplifier (to amplify the input ac signal from acoustic sensor) with a gain of 6 calculated using Eq. (2):

$$\text{Frequency} = \frac{1}{2\pi \cdot R1 \cdot C1} \tag{1}$$

$$\text{Gain} = 1 + \frac{R17}{R18} \tag{2}$$

Stage 2 functions as an isolation amplifier (galvanic isolation). Operator safety and signal quality of the acoustic sensors were ensured with isolated interconnections provided by the IL300 (high common mode rejection (130 dB) and high gain stability (± 0.005 %/°C)). In addition, it provides a barrier to avoid the generation of ground loops from the two groundings in the signal conditioning circuit. The isolation amplifier consists of inverting input and output. It amplifies the signal with a gain of 1.62. The gain was calculated based on the Eq. (3), where k2 is the output forward gain, k1 is the feedback transfer gain [16].

$$\text{Gain} = \frac{k2 \cdot (R5 + R6)}{k1 \cdot R20} \tag{3}$$

Stage 3 is a second order active low pass filter with a cut-off frequency of 1600 Hz, calculated using Eq. (4). The signal frequencies (from stage 2) that are greater than 1600 Hz were considered as the interference sounds and filtered in order to reduce the noise. Stage 3 was powered by power circuit_2.

$$\text{Frequency} = \frac{1}{2\pi^2 \sqrt{C11 \cdot C12 \cdot R8 \cdot R9}} \tag{4}$$
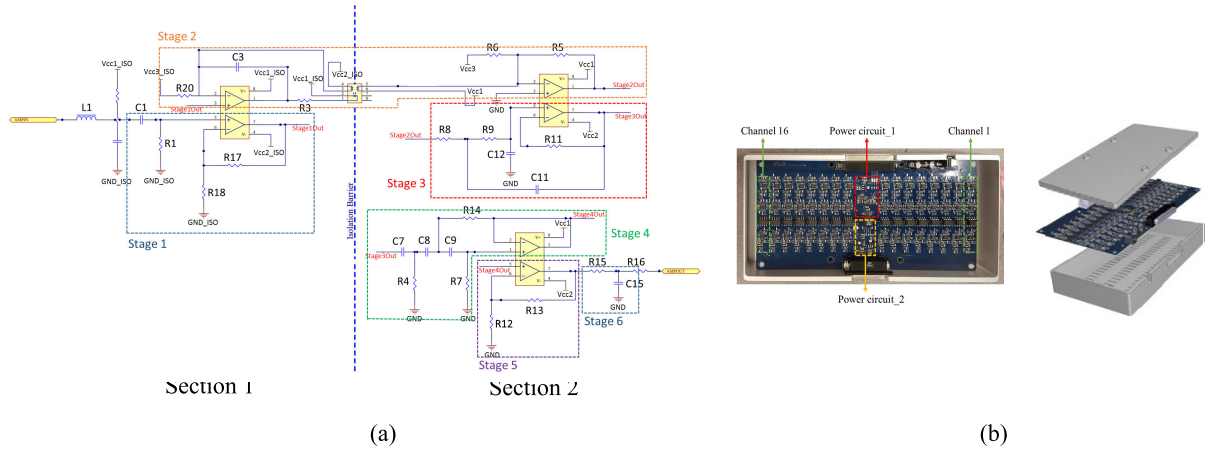
FIGURE 3. (a) The schematic of the single channel on signal conditioning circuit, (b) signal conditioning board with shield cover.

Stage 4 is a third-order active high pass filter with a cut-off frequency at 50 Hz, calculated using Eq. (5), and powered by power circuit_2. The signal frequencies from stage 3 that are lower than 50 Hz were considered as noises and filtered.

$$\text{Frequency} = \frac{1}{2\pi \sqrt[3]{C7 \cdot C8 \cdot C9 \cdot R4 \cdot R7 \cdot R14}} \quad (5)$$

Stage 5 is a non-inverting amplifier and amplifies the signal from stage 4 with a gain of 3.5 (Eq. (6)) and was powered by powered by power circuit_2.

$$\text{Gain} = 1 + \frac{R13}{R12} \quad (6)$$

Stage 6 is a first order passive low pass filter with cut-off frequency at 1600 Hz, calculated using Eq. (7), and is powered by powered by power circuit_2.

$$\text{Frequency} = \frac{1}{2\pi \cdot R15 \cdot C15} \quad (7)$$

Stage 1, stage 3, stage 4 and stage 6 together function as a band pass filter and an amplifier. In addition, two separate power distribution circuit developed with specific grounding was used for supply different input voltage for circuit of each channel (Figure 3(b), S2 and S3).

4) WIRELESS DATA ACQUISITION
Bluetooth 4.0 and Wi-Fi 802.11 (a, b, g, n) are widely used communication protocols for wireless data transmission. Even though Bluetooth offers better battery life with lower power consumption when compared to Wi-Fi, the data throughput, bit rate, and access range are lower for Bluetooth. In this work, the Wi-Fi based wireless transmission was chosen because the minimum raw bit rate required is 2.93 Mbps which can be achieved only by Wi-Fi communication (the HLT data recorded for a time period of 20 s required approximately 7.33 MB which is 0.3665 MB/s. This corresponds to a data transmission rate of 2.93 Mbps and was set as a minimum required transmission rate). Therefore, a compact and portable DAQ device (National Instruments (NI) 9205) along with a wireless chassis (NI 9191) was used to acquire

the analog signal from the signal conditioning circuit, convert to digital signal using in-built-in A/D converter and then wirelessly transmit the data reliably to a Wi-Fi enabled device such as a PC/tablet. This NI DAQ provides accurate wireless data transmission of multichannel signals with high transmission rate and no noticeable cross talk.

5) CUSTOM-BUILT LABVIEW AND MATLAB PROGRAM
A custom-built LabVIEW program was developed in the Wi-Fi enabled device (PC and tablet) to acquire the digital signals from the NI 9191 Wi-Fi module, which were converted and conditioned from HLT sounds detected by the acoustic sensors. In the LabVIEW program, the 'DAQ Assistant' function was used to select the data channels (1-16) and the sample rate, which was 8 kHz for one channel and 128 kHz for 16 channels. The 'Waveform Graph' function was used to display the real time waveform signals on the display screen. The 'Time Target' function was used to set the sound recording time of the stethograph system for 20 seconds to cover at least 4 breath cycles (based on a previously reported study by Gurung *et al.*, [35]). The 'Write to Measurement File' option was used to save the recorded data in a '.lvm' format database. The real time sound waveform detected by the 16 acoustic sensors was shown simultaneously on the custom built graphical user interface (GUI) (Fig. 4(a)) while the data was saved in '.lvm' file format.

A MATLAB program was developed to convert the recorded data from LabVIEW program into 16 audio files of '.WAV' format (for audio playback) (Fig. 4(b)) and audio for analyzing the heart and the lung conditions by visual examination. In addition, another MATLAB program was developed with algorithms and it has the capability to analyze the acquired data off-line and provides the information on HLT sounds including heartbeat and respiration rate to a physician/doctor and serves as an efficient tool in CCD diagnosis and monitoring. The photograph of the multi-channel stethograph system is shown in Fig. S4.
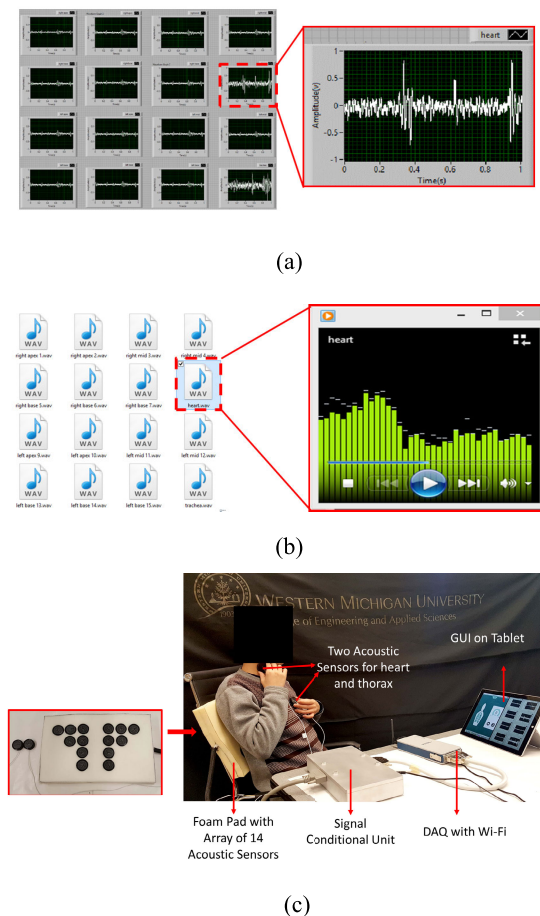
(a)

(b)

(c)

FIGURE 4. (a) LabVIEW program interface showing the real time sound waveforms, (b) MATLAB program converted digital data to 16.WAV audio file format, (c) measurement setup.

C. EXPERIMENT SETUP

Figure 4(c) shows the experiment setup of multi-channel stethograph system. The data (HLT sounds) was recording at the Center for Advanced Smart Sensors and Structures, Western Michigan University, USA. All the volunteers (above the age of 18 years) were seated, and the high density foam pad with 14 acoustic sensors was placed between the chest (behind/backside of the chest) and the backrest, one acoustic sensor was placed on the heart and the other sensor was placed on the side of the windpipe or trachea (Fig. 4(c)). The duration of each recording was set to 20 seconds for validating the functionality of the system by measuring HLT sound. The accuracy of vital sign measurement using the wireless stethograph system was validated by verifying the functionality of each component of the system individually as well as a whole system.

The human subjects internal review board (HSIRB) at Western Michigan University affirmed that the HSIRB approval is not required for conducting this study since the HLT sound data was only used to demonstrate the working of the prototype and optimizing the system design. In addition, all the subjects provided the written informed consent to participate in this study, and their personal information was not collected.

III. RESULTS AND DISCUSSION

A. CHARACTERIZATION OF MULTI-CHANNEL STETHOGRAPH SYSTEM

1) CHARACTERIZATION OF SIGNAL CONDITIONING CIRCUIT

Initially, to verify the amplification gain, 34, of designed signal conditioning circuit, its schematic was implemented in Pspice simulation software. A frequency of 1 kHz and a voltage of 0.1 V_{pk} was provided as input signal to the circuit and an output of 3.4 V_{pk} was obtained that results in a gain of 34. Later, the amplification gain of each channel of the fabricated signal conditioning board was measured by providing an input signal with a frequency of 1 kHz and a voltage of 0.1 V_{pk} using R.S.R FS-30 function generator. An average output signal of 3.36 $\pm$ 0.07 V_{pk} with gain of 33.6 was measured for the 16 channels of conditioning board on TDS5104B digital phosphor oscilloscope (Fig. 5(a), Fig. S5 and Fig. S6). This clearly shows that the designed signal conditioning circuit can provide a constant output signal in all the 16 channels with a desired amplification gain of $\sim$34. The ground pin of the oscilloscope was removed during measurements to avoid the generation of ground loops as well as the interference across the isolation barrier.

To characterize the filtering capability (noise reduction) of the fabricated signal conditioning board, an input signal with frequency ranging from 1 to 4000 Hz was applied to each channel using an Analog Discovery 2 USB logic analyzer. The output frequency response of the board was recorded and analyzed using Digilent Adept 2 software. Figure 5(b) shows the output frequency response of one of the channels (channel 1). The input signal with frequencies between 50 Hz to 1600 Hz were passed through the filters and amplified with gain $\sim$34 whereas the frequency signals outside this range were attenuated (results in relatively lower gain).

2) CHARACTERIZATION OF DAQ SYSTEM

The functionality of DAQ system, which includes DAQ device (A/D signal conversion), Wi-Fi communication (data transmission) and custom-built LabVIEW program (data recording) was validated by comparing the similarity between the output analog signal of signal conditioning board and the digital signal data recorded from LabVIEW program. Initially, a signal with the frequency of 1 kHz and voltage of 0.1 V_{pk} was applied as input to the signal conditioning board using the function generator, and the analog output of signal conditioning board output was measured and recorded using the digital oscilloscope. The analog output of signal conditioning board was then provided as input to the DAQ device integrated with Wi-Fi module. Following this, the digital output signal of DAQ device which was transferred to a Wi-Fi enabled PC and recorded by the LabVIEW program was compared with the analog output signal of the conditioning board using the cross-correlation algorithm implemented
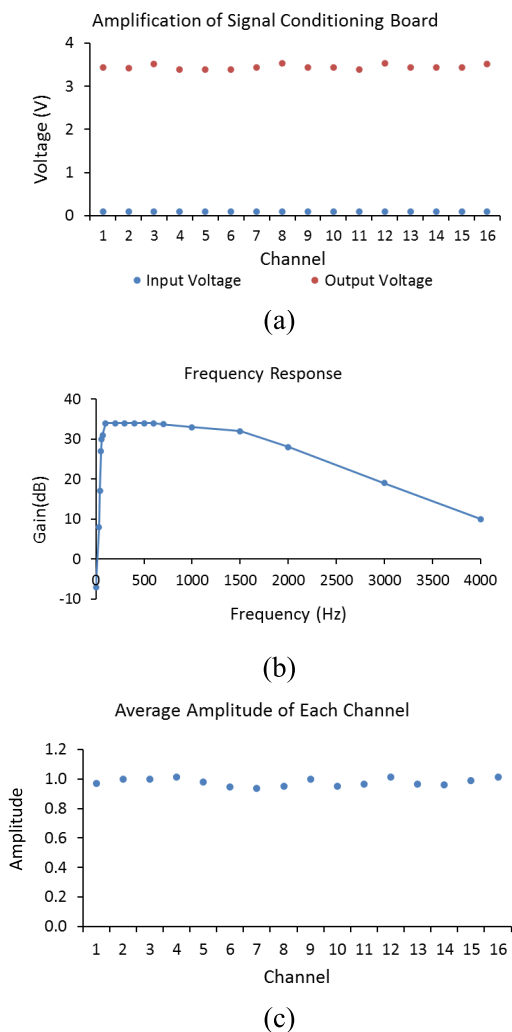
Amplification of Signal Conditioning Board

Frequency Response

Average Amplitude of Each Channel

FIGURE 5. (a) Amplification gain of signal condition circuit. (b) frequency response of signal conditioning circuit, (c) output voltages of the 16 acoustic sensors.

in MATLAB program. The result shows a correlation coefficient of 0.96 which indicates that the data acquisition system converts the signals from signal conditioning board and communicates to PC as intended.

3) CHARACTERIZATION OF ACOUSTIC SENSOR

The performance of the 16 acoustic sensors was validated by detecting sound signal with a constant frequency and comparing their output voltage amplitudes that were recorded on LabVIEW program using MATLAB. Initially, an acoustic sensor (before embedding into foam pad) connected to the channel 1 of the conditioning board (conditioning board was connected to DAQ system) was placed in front of a speaker that was playing a constant 1000 Hz audio. The output voltage of the acoustic sensor was recorded using LabVIEW. Similarly, the output voltages of the other 15 acoustic sensors were recorded. Average amplitude value of each output voltage signal of acoustic sensor from LabVIEW was calculated based on peak detection algorithm using MATLAB.

TABLE 2. Signal to noise ratio of STG system and clinicloud stethoscope.

	HLT Sounds			Ambient Sounds	
Sound Type	SNR (dB)		Sound Type	SNR (dB)	
	STG	CliniCloud		STG	CliniCloud
Heartbeat	23.6	16.7	Crying	16.5	30.3
Trachea	24.2	23.2	Laughing	23.7	31.1
Lung	12.1	10.4	Speaking	12.6	21.8

The calculated average amplitude of all 16 sensors was 0.98 ± 0.03 (Fig. 5(c)). The small standard deviation value indicates that the fabricated acoustic sensors have the same performance.

4) COMPARISON WITH COMMERCIAL ELECTRONICS STETHOSCOPE

The performance of the multi-channel stethograph (STG) system was investigated by recording HLT sounds and common sounds from ambient environment and comparing the signal to noise (SNR) ratios with CliniCloud Digital Stethoscope (FDA approved commercially available stethoscope) from CliniCloud Inc.

20 sets of HLT sounds (20 heartbeat, 20 trachea and 20 lung sound) were recorded from 10 healthy people using one channel (channel #8) of STG system and CliniCloud digital stethoscope for fair comparison purpose. MATLAB program was used for plotting the time waveform of the data collected from the system and CliniCloud digital stethoscope. Figure S7, S8 and S9 shows the example of HLT sound of a person measured using the developed stetograph system and digital stethoscope. It was observed that the waveforms in Fig. S7(a), S8(a) and S9(a) has higher signal amplitude and lower noise when compared to Fig. S7(b), S8(b) and S9(b). The average SNR of heartbeat, trachea and lung sound from 10 persons is 23.6 dB, 24.2 dB and 12.1 dB for STG system, respectively. Similarly, a SNR of 16.7 dB, 23.2 dB and 10.4 dB was measured for HLT sounds using CliniCloud digital stethoscope (Table 2). SNR results demonstrated that the STG system has better performance in measuring and recording HLT sound when compared to the commercial device.

The performance of the STG system and digital stethoscope was also evaluated with background sound sources, which include crying, laughing, and speaking. Initially, an STG system's acoustic sensor (channel 8 which is not embedded in foam pad) was placed in the front of a smartphone speaker that was playing a crying, laughing and speaking sound from YouTube. The same procedure was repeated with a digital stethoscope. The crying sound recorded by STG system (Fig. S10(a1)) and digital stethoscope (Fig. S10(b1)
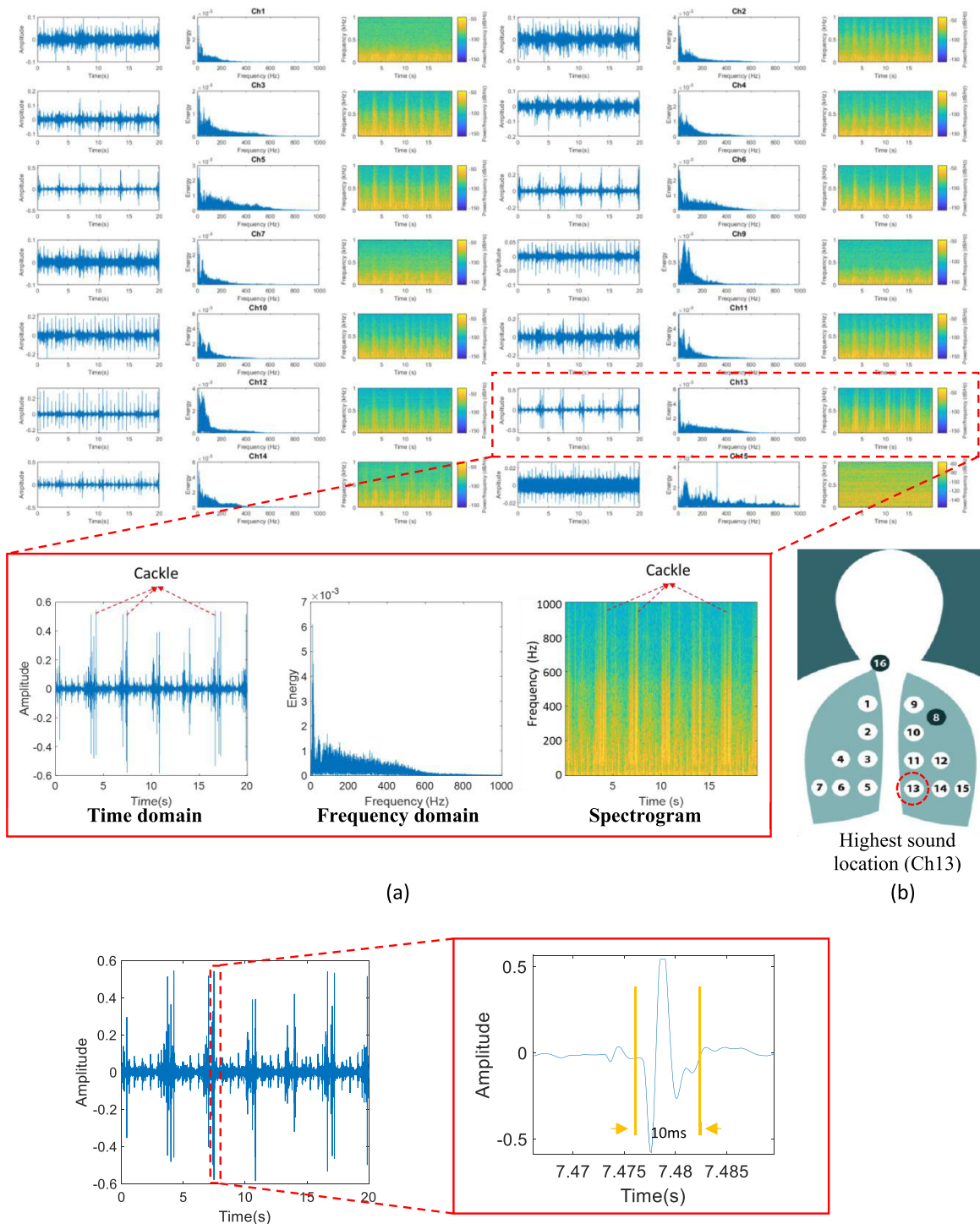
FIGURE 6. (a) Lung sounds with crackle in time domain, frequency domain and spectrogram, (b) origin of crackle location, (c) lung sound with crackle in time domain showing the time duration of crackle.

has a SNR of 16.5 dB and 30.3 dB, respectively. The laughing and speaking sounds recorded by STG system (Fig. S10(a2,a3)) and digital stethoscope (Fig. S10(b2,b3)) has a SNR of 23.7 dB and 31.1 dB; 12.6 dB and 21.8 dB, respectively. The result indicated that the STG system has better filtering capability due to the lower SNR value.

B. DIGITAL SIGNAL PROCESSING OF SOUND DATA

1) IDENTIFICATION OF ABNORMALITIES IN LUNG SOUNDS (VISUALIZATION OF LUNG SOUNDS)

Crackle, rhonchi and wheeze are the most common abnormalities in the CCD [35]. The traditional stethoscopes cannot provide information on the frequency and time distribution
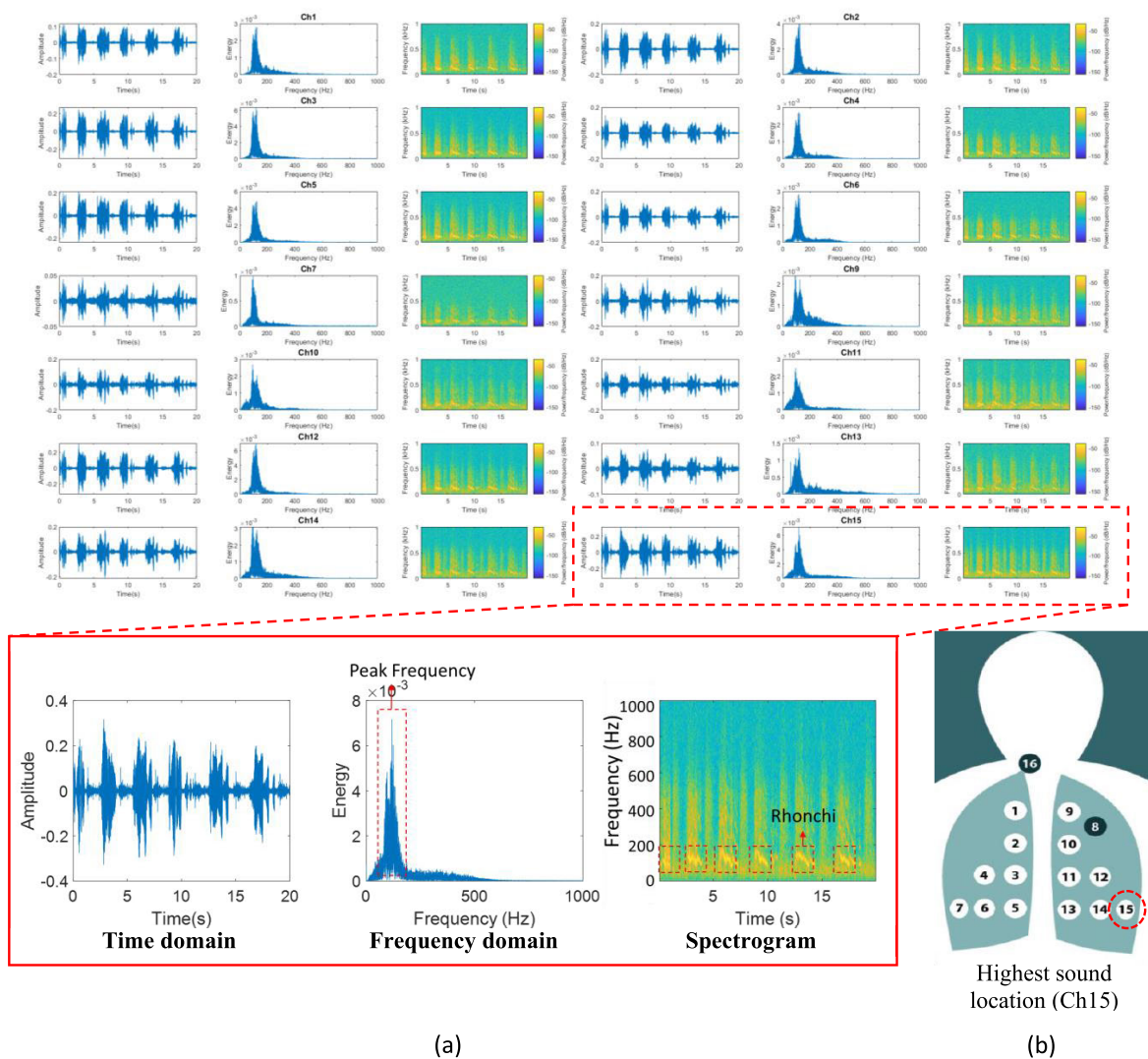
FIGURE 7. (a) Lung sound with rhonchi in time domain, frequency domain and spectrogram, and (b) origin of rhonchi location.

of these adventitious sounds but only facilitates the physician/doctor to manually hear them. Therefore, it is very difficult to accurately identify and distinguish crackles, rhonchi and wheeze as well as their origin location using the traditional stethoscopes. However, the developed multi-channel stethograph system was able to find the original location and type of the adventitious sounds as well as provides a visualization with all the information, including amplitude, frequency, count and duration of crackles, rhonchi, and wheeze in the time domain, frequency domain and spectrogram [36]–[39]. In order to demonstrate and validate the capability of the developed system, HLT audio recordings from verified patients with crackles, rhonchi and wheeze were collected by Stethographics Inc, Massachusetts, USA.

Crackle is a discontinuous clicking or rattling sound that is common in patients with pneumonia and congestive heart failure [38]. Crackle exhibits relatively higher amplitude

peaks when compared to rhonchi and wheeze with a time duration less than 50 ms (can be identified from sounds/audio in time domain) and has a frequency range between 100 Hz to 1600 Hz (can be identified from in spectrogram) [38]. Figure 6(a) shows the crackles in time domain, frequency domain and spectrogram and Fig. 6(b) shows the location of the mother crackle sound collected by the channel 13 of the stethograph system (since the location of channel 13 provided highest amplitude and most clear pattern in time domain). Crackles were identified in the time domain of the recorded audio based on the peaks of the amplitude (approximately -0.6 to $+0.6$) and time duration of the narrow peaks ($\sim$10 ms) (Fig. 6(a)(c)). In addition, the frequency distribution of the recorded audio in spectrogram clearly shows that the range of the frequency were very wide (from $\sim$800 Hz to 1000 Hz, darker yellow lines). Based on the time domain and spectrogram results, it is clearly evident that the abnormal sound in the audio is nothing but crackles.
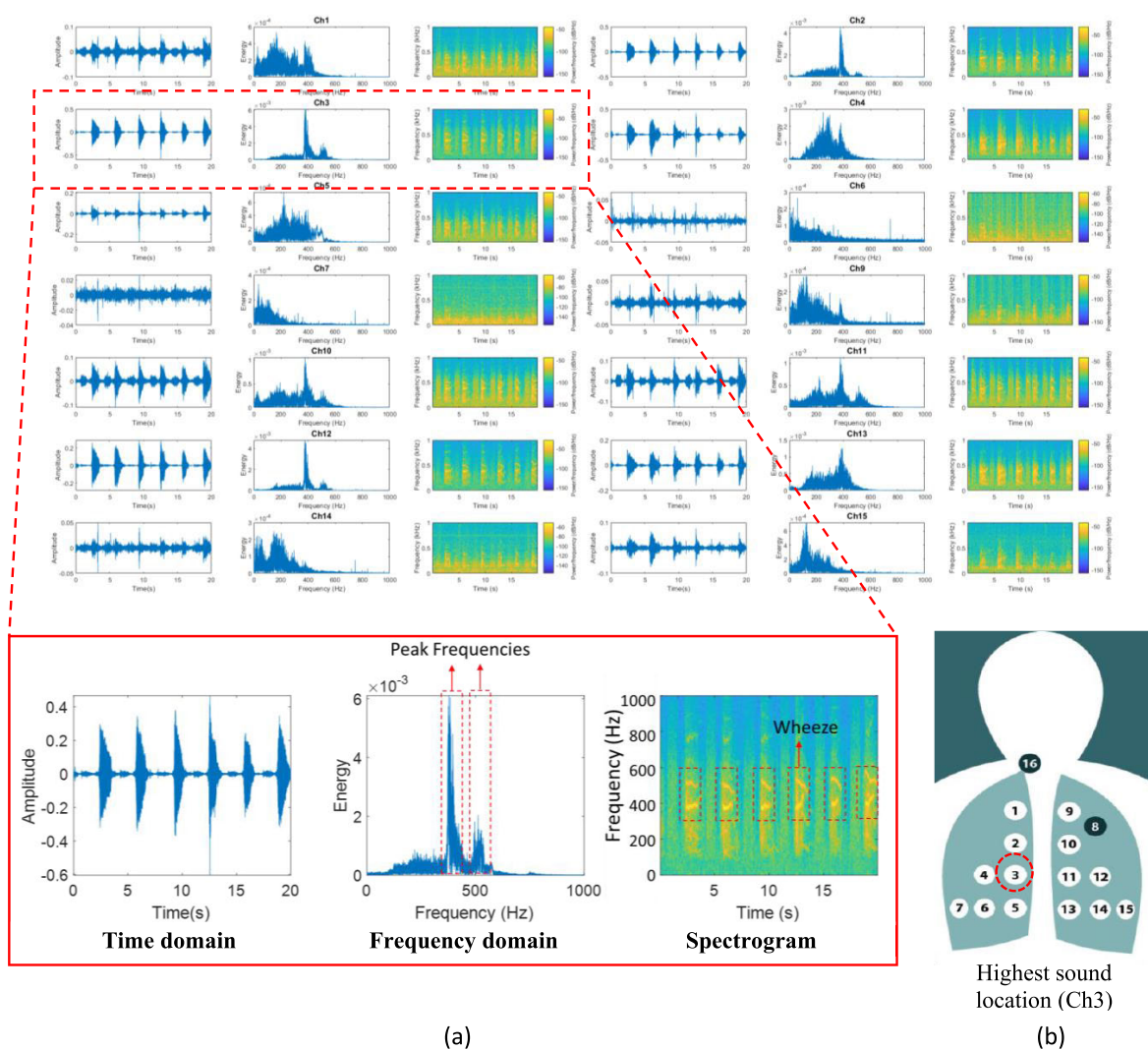
FIGURE 8. (a) Lung sound with wheeze in time domain, frequency domain and spectrogram, and (b) origin of wheeze location.

Rhonchi is a low-pitched, continuous sound and can be found in patients with COPD, bronchiectasis, pneumonia, chronic bronchitis and cystic fibrosis. Rhonchi has a frequency approximately ≤ 250 Hz (can be identified in frequency domain and spectrogram) and a time duration > 250 ms (can be identified in spectrogram) [39]. Figure 7(a) shows the rhonchi in time domain, frequency domain and spectrogram and Fig. 7(b) shows the location of the mother rhonchi sound collected by the channel 15. The Peak/dominant frequency of the audio was observed at ~ 150 Hz in the frequency domain and spectrogram. The rhonchi is a continuous sound and in spectrogram, it is clearly observed that the time duration of the prominent pattern (darker yellow region) is >1s.

Wheeze is a high-pitched, continuous sound. It is common in several diseases such as COPD, asthma, lung cancer, congestive heart failure. Wheeze has a frequency approximately equal or >400 Hz (can be identified in frequency domain and spectrogram) and time duration >250 ms (can be identified in

spectrogram) [36], [37]. Figure 8(a) shows the wheeze in time domain, frequency domain and spectrogram and Fig. 8(b) shows the location of the mother wheeze sound collected by the channel 3. In the recorded audio from channel 3, there were wheezes located at different frequencies of 400 Hz and 500 Hz as shown in the frequency domain. Similarly, these different frequencies of the wheeze were identified in spectrogram and it was noticed that they were overlapping since they occurred/generated at same time. The results clearly demonstrated that the developed system has the capability to identify and distinguish the abnormal sounds such as crackles, rhonchi and wheeze, and aid the physician/doctor in better diagnosis of the patient for CCD.

2) RESPIRATION AND HEART RATE DETECTION ALGORITHMS

In addition to abnormalities in lung sounds, heartbeat rate and respiratory rate are other important factors required for CCD monitoring and diagnosis. However, it is difficult to observe
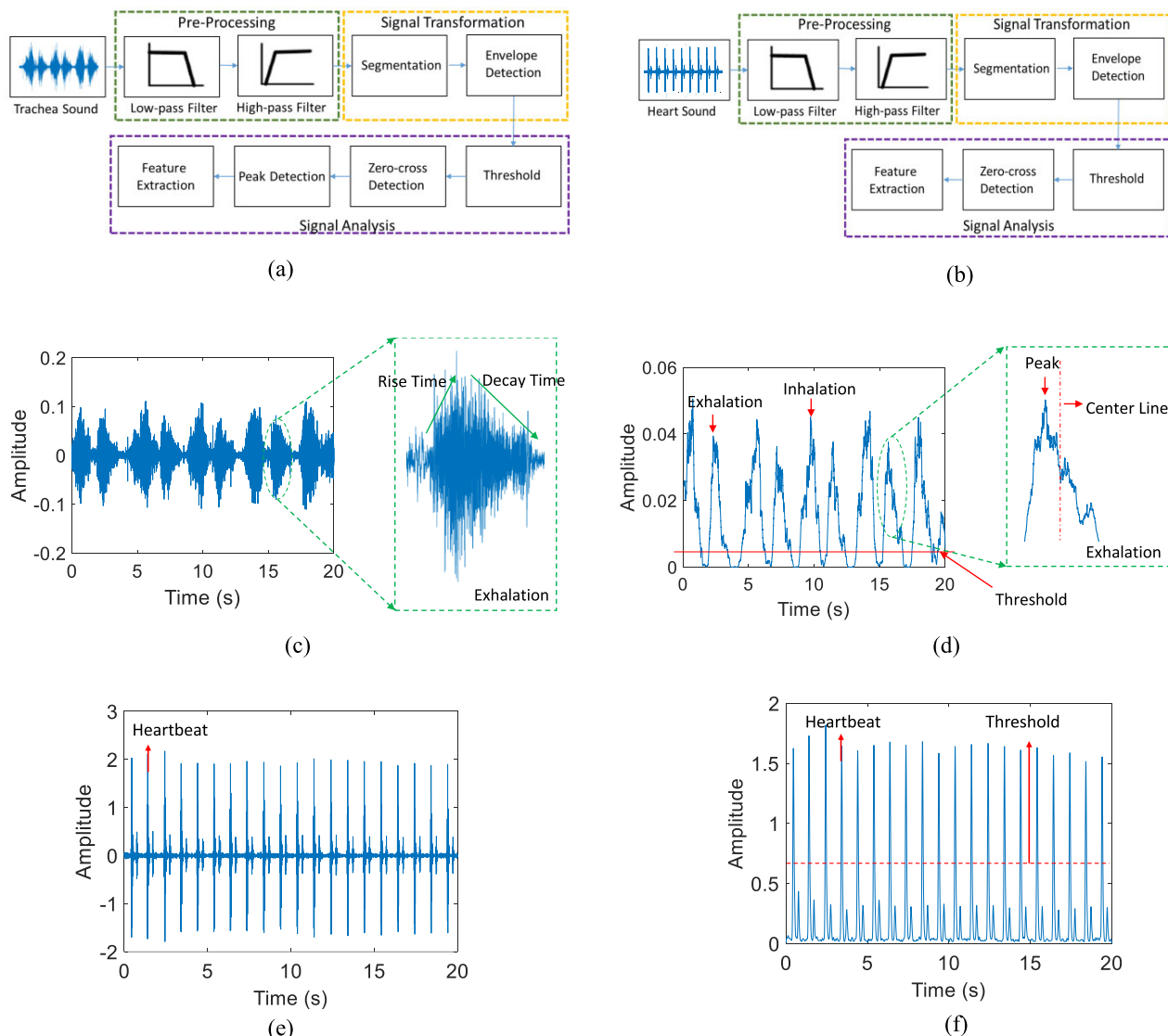
FIGURE 9. (a) Block diagram of respiration rate detection algorithm, (b) block diagram of heart rate detection algorithm, (c) trachea sound in time domain, (d) processed trachea sound in time domain, (e) heart audio in time domain and (f) processed heart audio in time domain.

or manually identify/measure respiration and heartbeat rate directly from visualized lung sound. To overcome this problem, two dedicated sensors are used along with digital signal processing (DSP) methods for developing algorithms that can automatically measure respiration (inhalation and exhalation) and heartbeat rate which further ease physician/doctor in CCD diagnosis.

a: RESPIRATION RATE DETECTION ALGORITHM

The algorithm for detecting the respiration rate includes three stages consisting of pre-process, signal transformation, and signal analysis (Fig. 9(a)). Typically, respiration rates (inhalation and exhalation) has been detected using lung sound [40]–[47]. However, lung sounds are relatively small and has noises from heartbeat and blood vessels. Trachea sound is louder when compared to lung sound, contains

less noise from the body and thus provides clear respiration patterns [48].

Initially, pre-process stage was required to ensure that all high-frequency and low frequency noise artifacts from environment as well as body were eliminated. This was achieved by employing a bandpass filter (passband of 50 Hz and stopband of 180 Hz) with no time shift in data processing using zero-phase digital filtering technique. Since sound is an oscillating signal with complexed pattern, the parameters of inhalation and exhalation were identified using time expanded waveform analysis and then the signal transformation was performed by segmentation and envelope detection techniques to convert the signal in time waveform to a smooth curve (Fig. 9(c)). This was implemented by moving a hamming window with size 100 (at 8000 samples per second) and 50% overlapping at the absolute value of the trachea signal.

The smooth curve of trachea signal was then analyzed by using threshold, zero-cross, peak detection, and feature extraction techniques (Fig. 9(d)). The threshold detection technique was used for inhalation and exhalation signal extraction. Typically, the amplitude of the recorded sound signals vary from one human subject to another due to numerous factors such as the size of lungs, health condition, age, and gender. Thus, a dynamic threshold for the amplitude was determined empirically, and the best result occurred at 10% of the mean peak value detected by peak detection technique was considered as the threshold of the amplitude. Every cycle with magnitude greater than 10% of the mean peak value of the time waveform was considered to be a breath (can be either inhalation or exhalation) when the threshold is applied. Then each of the breath pattern was extracted using zero-crossing method. Finally, the extracted breath patterns are verified by a set of criteria to improve the accuracy. Respiration rate was mathematically calculated using Eq. (8):

$$\text{Respiration rate} = \frac{N}{T} \times 60 \qquad (8)$$

where N is number of the breaths that were extracted and T is the total duration of the trachea sound in seconds. The rising time is longer than decay time in inhalation and shorter in exhalation, and this helps in identifying the inhalation and exhalation patterns in the trachea sound [49]. In addition, a peak detection method was used for determining the location of the breath peak and in calculating the rise and decay times for identifying inhalation and exhalation.

b: HEARTBEAT DETECTION ALGORITHM

The algorithm for detecting the heart rate from the recorded heart sound in time waveform was implemented in three stages (pre-process, signal transformation, and signal analysis) and includes techniques such as hamming window, envelop, peak detection and threshold (Fig. 9(b)). Figure 9(e) shows the raw data of the heart signal. In pre-process stage, a bandpass filter (passband of 180 Hz and stopband of 300 Hz) with zero-phase digital filtering technique was used to filter unwanted sounds such as breath sound and white noise. In signal transformation stage, a smooth curve of heart signal was generated from its absolute value using a moving Hamming window with size 100 (at 8000 samples per second) and a 50% overlap. Each heartbeat includes a high and short amplitude peak, and a peak detection technique was used for determining all the peaks (irrespective of the amplitude of the heart signal). During signal analysis stage, a dynamic threshold value was obtained by calculating the average of all the peaks and peaks with magnitude greater than threshold value was considered to be high peaks. Each high peak represents one heartbeat (Fig. 9(f)). Also, all the peaks are verified by a set of criteria. In addition, heartbeat rate can be calculated based on the duration of the heart signal and the number of high peaks/heartbeats in the signal.

TABLE 3. Evaluation of respiration and heartbeat rate detection algorithms.

Parameter	Sample	TP	FN	FP	SE (%)	PPV (%)
Respiration Rate	40	38	2	0	95	100
Heartbeat Rate	40	36	3	1	92	97

c: EVALUATION OF ALGORITHMS

The overall performance of the developed algorithms have been evaluated based on the 40 sets of HLT sound data collected from 10 healthy people with the multi-channel stethograph system. From experimental data, three quantitative results were computed: true positive (TP) when a respiration and heartbeat segment is correctly detected, false negative (FN) when a respiration and heartbeat segment is not detected, and false positive (FP) when a noise segment is detected as either a respiration or heartbeat segment. The performance metrics are show in Table 3. The developed algorithm obtained an average sensitivity (SE) of 95% and 92% for the measurement of respiration and heartbeat rate, respectively (calculated using Eq. (9)). High positive predictive value (PPV(%)) was calculated which indicates that no or low noise was detected as a respiration or heartbeat (Eq. (10)).

$$SE\ (\%) = \frac{TP}{TP + FN} \times 100\% \qquad (9)$$

$$PPV\ (\%) = \frac{TP}{TP + FP} \times 100\% \qquad (10)$$

Therefore, it can be concluded that the developed wireless stethograph system can serve as an effective and efficient tool to physician or doctor to quantify the abnormalities present in the HLT sound.

IV. CONCLUSION

A multi-channel stethograph system was successfully developed to record and plot HLT sounds non-invasively through a set of 16 acoustic sensors. It has overcome the limitations of current stethoscope systems and has an advanced signal conditioning board with Wi-Fi communication functionalities for detecting, conditioning and transmitting HLT sounds simultaneously. The recorded audio files and plotted waveforms of the HLT sounds demonstrated the capability of employing the multi-channel stethograph system for visual examination of any abnormal patterns in inhalation and exhalation thus providing information to physicians which helps in analyzing the heart and the lungs condition and diagnosing CCD. The STG system provides various benefits including improved quality of care and clinical productivity through faster testing particularly when X-Rays or CAT scans are to be avoided; increased physician productivity through the immediate display of results vs X-Ray delays; cost savings from decreased use of X-Rays, echocardiographs, and other tests; lower risk of misdiagnosis by the visualization of sound waves, the automated counting of wheezes, crackles and other sounds and

through the use of reference materials and sound samples. The future work is focused on performing the clinical studies by coordinating with hospitals and developing the algorithms as well as a graphical user interface (GUI) to automatically correlate the abnormalities in the HLT sounds to CCDs to further aid the physician/doctor in better diagnosis.

REFERENCES

[1] *Top 20 Pneumonia Facts-2019, American Thoracic Society*: Accessed: Oct. 9, 2020, [Online]. Available: https://www.thoracic.org/patients/patient-resources/resources/top-pneumonia-facts.pdf

[2] COPD. *Centers for Disease Control and Prevention*. Accessed: Oct. 9, 2020, [Online]. Available: https://www.cdc.gov/dotw/copd/index.html#:~:text=COPD%20affects%20more%20than%2015,smoke%20and%20other%20air%20pollutants

[3] *Heart Failure Statistics, Emory Healthcare*. Accessed: Oct. 9, 2020. [Online]. Available: https://www.emoryhealthcare.org/heart-vascular/wellness/heart-failure-statistics.html

[4] B. Hasse, M. M. Hannan, P. M. Keller, F. P. Maurer, R. Sommerstein, D. Mertz, D. Wagner, N. Fernández-Hidalgo, J. Nomura, V. Manfrin, and D. Bettex, ''International society of cardiovascular infectious diseases guidelines for the diagnosis, treatment and prevention of disseminated *Mycobacterium chimaera* infection following cardiac surgery with cardiopulmonary bypass,'' *J. Hospital Infection*, vol. 104, no. 2, pp. 214–235, 2020.

[5] COPD. (2020). *Pneumonia & Heart Failure, Study*. Accessed: Oct. 9, 2020, [Online]. Available: https://www.study.com/academy/lesson/copd-pneumonia-heart-failure.html

[6] (2020). *Breath Sounds, U.S. National Library of Medicine*. Accessed: Oct. 9, 2020. [Online]. Available: https://medlineplus.gov/ency/article/007535.htm

[7] A. Vyshedskiy, F. Bezares, R. Paciej, M. Ebril, J. Shane, and R. Murphy, ''Transmission of crackles in patients with interstitial pulmonary fibrosis, congestive heart failure, and pneumonia,'' *Chest*, vol. 128, no. 3, pp. 1468–1474, Sep. 2005.

[8] P. Leijdekkers and G. Valerie, ''Personal heart monitoring system using smart phones to detect life threatening arrhythmias,'' in *Proc. CBMS*, Jun. 2006, pp. 157–164.

[9] R. L. H. Murphy, S. K. Holford, and W. C. Knowler, ''Visual lung-sound characterization by time-expanded wave-form analysis,'' *New England J. Med.*, vol. 296, no. 17, pp. 968–971, Apr. 1977.

[10] L. Scalise, ''Non-contact heart monitoring,'' *Adv. EKG-Meth. Anal.*, vol. 8, pp. 81–106, Jan. 2012.

[11] R. Loudon and M. J. Raymond, ''Lung sounds,'' in *The Lung: Scientific Foundations*, vol. 1, 2nd ed., R. G. Crystal *et al.*, Eds. New York, NY, USA: Raven Press, 1997, pp. 663–673.

[12] R. Loudon and R. L. Murphy, Jr., ''Lung sounds,'' *Am. Rev. Respir. Dis.*, vol. 130, no. 4, pp. 663–673, 1984.

[13] E. Messner, M. Hagmuller, P. Swatek, F.-M. Smolle-Juttner, and F. Pernkopf, ''Respiratory airflow estimation from lung sounds based on regression,'' in *Proc. IEEE Int. Conf. Acoust., Speech Signal Process. (ICASSP)*, Mar. 2017, pp. 1123–1127.

[14] S. G. Wong, ''Design, characterization and application of a multiple input stethoscope apparatus,'' M.S. thesis, Dept. Elect. Eng., California Polytech. State Univ., San Luis Obispo, CA, USA, 2014, pp. 1–157.

[15] W.-C. Su, Y. Chen, and J. Xi, ''A new approach to estimate ultrafine particle respiratory deposition,'' *Inhalation Toxicol.*, vol. 31, no. 1, pp. 35–43, Jan. 2019.

[16] N. Sahgal, ''Monitoring and analysis of lung sounds remotely,'' *Int. J. Chron. Obstruct. Pulmon. Dis.*, vol. 6, no. 6, pp. 407–412, 2011.

[17] S. Charleston-Villalobos, G. Martinez-Hernandez, R. Gonzalez-Camarena, G. Chi-Lem, J. G. Carrillo, and T. Aljama-Corrales, ''Assessment of multichannel lung sounds parameterization for two-class classification in interstitial lung disease patients,'' *Comput. Biol. Med.*, vol. 41, no. 7, pp. 473–482, Jul. 2011.

[18] M. A. Islam, I. Bandyopadhyaya, P. Bhattacharyya, and G. Saha, ''Multichannel lung sound analysis for asthma detection,'' *Comput. Methods Programs Biomed.*, vol. 159, pp. 111–123, Jun. 2018.

[19] S. H. Li, B. S. Lin, C. H. Tsai, C. T. Yang, and B. S. Lin, ''Design of wearable breathing sound monitoring system for real-time wheeze detection,'' *Sensors*, vol. 17, no. 1, pp. 171–186, 2017.

[20] G. Karacocuk, F. Höflinger, R. Zhang, L. M. Reindl, B. Laufer, K. Möller, M. Röell, and D. Zdzieblik, ''Inertial sensor-based respiration analysis,'' *IEEE Trans. Instrum. Meas.*, vol. 68, no. 11, pp. 4268–4275, Nov. 2019.

[21] M. T. La Rovere, G. D. Pinna, R. Maestri, A. Mortara, S. Capomolla, O. Febo, R. Ferrari, M. Franchini, M. Gnemmi, C. Opasich, and P. G. Riccardi, ''Short-term heart rate variability strongly predicts sudden cardiac death in chronic heart failure patients,'' *Circulation*, vol. 107, no. 4, pp. 565–570, Feb. 2003.

[22] N. Ambrosino, C. Opasich, P. Crotti, F. Cobelli, L. Tavazzi, and C. Rampulla, ''Breathing pattern, ventilatory drive and respiratory muscle strength in patients with chronic heart failure,'' *Eur. Respiratory J.*, vol. 7, no. 1, pp. 17–22, Jan. 1994.

[23] R. R. Rodriguez, ''Toward a consensus definition for COPD exacerbations,'' *Chest*, vol. 117, no. 5, pp. 398–401, 2000.

[24] A. Vyshedskiy, R. M. Alhashem, R. Paciej, M. Ebril, I. Rudman, J. J. Fredberg, and R. Murphy, ''Mechanism of inspiratory and expiratory crackles,'' *Chest*, vol. 135, no. 1, pp. 156–164, Jan. 2009.

[25] T. G. Ferguson, ''Recommendations for the management of COPD,'' *Chest*, vol. 117, no. 2, pp. 23–28, 2000.

[26] A. Malinovschi, J. A. Fonseca, T. Jacinto, K. Alving, and C. Janson, ''Exhaled nitric oxide levels and blood eosinophil counts independently associate with wheeze and asthma events in National Health and Nutrition Examination Survey subjects,'' *J. Allergy Clin. Immunol.*, vol. 132, no. 4, pp. 821–827, 2013.

[27] A. H. Bahrainwala and M. R. Simon, ''Wheezing and vocal cord dysfunction mimicking asthma,'' *Current Opinion Pulmonary Med.*, vol. 7, no. 1, pp. 8–13, Jan. 2001.

[28] M. S. Figueroa and I. P. Jay, ''Congestive heart failure: Diagnosis, pathophysiology, therapy, and implications for respiratory care,'' *Respir. Care*, vol. 51, no. 4, pp. 403–412, 2006.

[29] J. P. Metlay, N. K. Wishwa, and J. F. Michael, ''Does this patient have community-acquired pneumonia?: Diagnosing pneumonia by history and physical examination,'' *Jama*, vol. 278, no. 17, pp. 1440–1445, 1997.

[30] X. Zhang, B. B. Narakathu, D. Maddipatla, B. J. Bazuin, and M. Z. Atashbar, ''P1DH.10–Development of a novel wireless multichannel stethograph system for diagnosing pulmonary and cardiovascular diseases,'' in *Proc. IMCS*, 2018, pp. 673–674, doi: 10.5162/IMCS2018/P1DH.10.

[31] X. Zhang, B. B. Narakathu, D. Maddipatla, V. S. Turkani, B. J. Bazuin, and M. Z. Atashbar, ''Digital signal processing and analysis of cardiopulmonary audio using a multi-channel stethograph system,'' in *Proc. IEEE Sensors*, Oct. 2018, pp. 1–4, doi: 10.1109/ICSENS.2018.8589512.

[32] N. Gavriely, Y. Palti, G. Alroy, and J. B. Grotberg, ''Measurement and theory of wheezing breath sounds,'' *J. Appl. Physiol.*, vol. 57, no. 2, pp. 481–492, Aug. 1984.

[33] P. D. Stein, H. N. Sabbah, J. B. Lakier, D. J. Magilligan, and D. Goldstein, ''Frequency of the first heart sound in the assessment of stiffening of mitral bioprosthetic valves,'' *Circulation*, vol. 63, no. 1, pp. 200–203, Jan. 1981.

[34] M. Sarkar, I. Madabhavi, N. Niranjan, and M. Dogra, ''Auscultation of the respiratory system,'' *Ann. Thoracic Med.*, vol. 10, no. 3, pp. 158–168, 2015.

[35] A. Gurung, C. G. Scrafford, J. M. Tielsch, O. S. Levine, and W. Checkley, ''Computerized lung sound analysis as diagnostic aid for the detection of abnormal lung sounds: A systematic review and meta-analysis,'' *Respiratory Med.*, vol. 105, no. 9, pp. 1396–1403, Sep. 2011.

[36] S. Alsmadi and Y. P. Kahya, ''Design of a DSP-based instrument for real-time classification of pulmonary sounds,'' *Comput. Biol. Med.*, vol. 38, no. 1, pp. 53–61, Jan. 2008.

[37] R. Palaniappan, K. Sundaraj, and N. U. Ahamed, ''Machine learning in lung sound analysis: A systematic review,'' *Biocybern. Biomed. Eng.*, vol. 33, no. 3, pp. 129–135, 2013.

[38] A. L. Key, K. Holt, C. J. Warburton, P. P. Walker, and J. E. Earis, ''Use of zonal distribution of lung crackles during inspiration and expiration to assess disease severity in idiopathic pulmonary fibrosis,'' *Postgraduate Med. J.*, vol. 94, no. 1113, pp. 381–385, Jul. 2018.

[39] W. Y. Yan, L. Li, Y. G. Yang, X. L. Lin, and J. Z. Wu, ''Application of the computer-based respiratory sound analysis system based on Mel-frequency cepstral coefficient and dynamic time warping in healthy children,'' *Chin. J. Pediatrics*, vol. 54, no. 8, pp. 605–609, 2016.

[40] S. Shirmohammadi, K. Barbe, D. Grimaldi, S. Rapuano, and S. Grassini, ''Instrumentation and measurement in medical, biomedical, and healthcare systems,'' *IEEE Instrum. Meas. Mag.*, vol. 19, no. 5, pp. 6–12, Oct. 2016.

[41] A. Oliveira and A. Marques, ''Respiratory sounds in healthy people: A systematic review,'' *Respiratory Med.*, vol. 108, no. 4, pp. 550–570, Apr. 2014.

[42] M. M. Jaber, S. K. Abd, P. M. Shakeel, M. A. Burhanuddin, M. A. Mohammed, and S. Yussof, "A telemedicine tool framework for lung sounds classification using ensemble classifier algorithms," *Measurement*, vol. 162, pp. 107883–107890, Oct. 2020.

[43] A. Mondal, P. Bhattacharya, and G. Saha, "Detection of lungs status using morphological complexities of respiratory sounds," *Sci. World J.*, vol. 2014, pp. 2014–2023, Jan. 2014.

[44] M. Oud, "Lung function interpolation by means of neural-network-supported analysis of respiration sounds," *Med. Eng. Phys.*, vol. 25, no. 4, pp. 309–316, May 2003.

[45] H. Pasterkamp, R. E. Powell, and I. Sanchez, "Lung sound spectra at standardized air flow in normal infants, children, and adults," *Amer. J. Respiratory Crit. Care Med.*, vol. 154, no. 2, pp. 424–430, Aug. 1996.

[46] K. Ohkawa, Y. Masaru, and M. Shoichi, "Classification between abnormal and normal respiration through observation rate of heart sounds within lung sounds," in *Proc. IEEE EUSIPCO*, Sep. 2018, pp. 1142–1146.

[47] W. Xie, P. Gaydecki, and A.-L. Caress, "An inhaler tracking system based on acoustic analysis: Hardware and software," *IEEE Trans. Instrum. Meas.*, vol. 68, no. 11, pp. 4472–4480, Nov. 2019.

[48] T. Penzel and S. AbdelKebir, "The use of tracheal sounds for the diagnosis of sleep apnoea," *Breath.*, vol. 13, no. 2, pp. 37–45, 2017.

[49] J. Castro and P. Marti-Puig, "Real-time identification of respiratory movements through a microphone," *Adv. Distrib. Comput. Artif. Intell. J.*, vol. 3, no. 3, pp. 64–75, 2014.

XINGZHE ZHANG (Member, IEEE) received the B.S. degree in electronics engineering from Mapúa University, Manila, Philippines, in 2014, and the M.Sc. degree in electrical engineering from Western Michigan University, Kalamazoo, USA, in 2017, where he is currently pursuing the Ph.D. degree in electrical engineering. He is also a full-time Research Assistant with the Center for Advanced Smart Sensors and Structures, Department of Electrical and Computer Engineering. His research interests include design and fabrication of sensor, design of sensor systems, and developing digital signal processing algorithm.

DINESH MADDIPATLA (Member, IEEE) received the B.E. degree in electrical and electronics engineering from Anna University, India, in 2013, and the M.Sc. degree in electrical engineering and the Ph.D. degree in electrical and computer engineering from Western Michigan University, Kalamazoo, USA, in 2016 and 2020, respectively. He is currently working as a Research Associate with the Centre for Advanced Smart Sensors and Structures (CASSS), Western Michigan University. He has published over 70 refereed journal articles and refereed conference proceedings. In addition, he has published over 15 patents and invention disclosures. His research interests include all aspects of design, fabrication, and characterization of printed electronics, focusing on flexible sensor structures, microfluidics, electrochemical sensors, gas sensors, and lab-on-a-chip sensing systems. He was awarded the Technology Transfer Talent Network (T3N) from the State of Michigan, the All-University Research and Creative Scholar Award, and the Dissertation Completion Fellowship from Western Michigan University. He is also serving as a reviewer for more than 15 international journals.

BINU B. NARAKATHU (Member, IEEE) received the B.E. degree in electronics and communication engineering from Visvesvaraya Technological University, Bengaluru, India, the M.Sc. degree in computer engineering from Western Michigan University, USA, in 2009, and the Ph.D. degree from the Department of Electrical and Computer Engineering, Western Michigan University, in 2014. From 2015 to 2017, he was a Postdoctoral Fellow with the Sensor Technology Laboratory (STL), Department of Electrical and Computer Engineering, Western Michigan University, where he is currently a Research Associate with the Center for Advanced Smart Sensors and Structures (CASSS), Department of Electrical and Computer Engineering. He has published over 140 refereed journal articles and refereed conference proceedings. In addition, he has published ten patents and more than 30 invention disclosures. His research interests include all aspects of design, fabrication, and characterization of high-performance sensing systems, microfluidic devices, lab-on-a-chip for point-of-care testing (POCT), biosensors, bioelectronics, printed electronic devices, and BioMEMS devices for applications in the biomedical, environmental, and defense industries. He is serving as a member of the Technical Council Committee for NextFlex and a DoD Funded Consortium for Flexible Hybrid Electronics.

BRADLEY J. BAZUIN (Member, IEEE) received the B.S. degree in electrical engineering from Yale University, New Haven, CT, USA, in 1980, and the M.S. and Ph.D. degrees in electrical engineering from Stanford University, Stanford, CA, USA, in 1982 and 1989, respectively. He was a Research Assistant with the Center for Integrated Electronics in Medicine associated with the Integrates Circuits Laboratory, the Center for Integrated Systems, Stanford University, from 1981 to 1988. He was a part-time MTS and System Engineer, from 1981 to 1989; a Principal Engineer with ARGOSystems, Sunnyvale, CA, USA, from 1989 to 1991; and a Senior Systems Engineer with Radix Technologies, Mountain View, CA, USA, from 1991 to 2000. He has been a Term Appointed Assistant Professor and an Assistant Professor with Western Michigan University, Kalamazoo, MI, USA, since 2000, where he is currently an Associate Professor of electrical and computer engineering. His current research interests include printed electronics, electronic and printed circuit board circuit design and fabrication, custom integrated circuit design, embedded signal processing, wireless communication, software defined radios, and advanced digital signal processing algorithms for physical layer communication systems. He is a member of American Society for Engineering Education and the Institute of Navigation.

MASSOOD Z. ATASHBAR (Senior Member, IEEE) received the B.Sc. degree in electrical engineering from Isfahan University of Technology, Isfahan, Iran, the M.Sc. degree in electrical engineering from Sharif University of Technology, Tehran, Iran, and the Ph.D. degree from the Department of Communication and Electronic Engineering, Royal Melbourne Institute of Technology University, Melbourne, Australia, in 1998. From 1998 to 1999, he was a Postdoctoral Fellow with the Center for Electronic Engineering and Acoustic Materials, The Pennsylvania State University, University Park, USA. He is currently a Professor with the Electrical and Computer Engineering Department and the Founding Director of the Center for Advanced Smart Sensors and Structures (CASSS), Western Michigan University, USA. He has published over 280 refereed articles, refereed conference proceedings, and four book chapters. In addition, he has published ten patents and more than 30 invention disclosures. His research interests include physical and chemical sensor development, wireless sensors, and applications of nanotechnology in sensors and flexible hybrid electronic devices. He was a member of the editorial board. He is serving as a Lead Member of the Technical Council Committee and the Co-Chair of the Technical Working Group (TWG) for NextFlex, and a DoD Funded Consortium for Flexible Hybrid Electronics. He was an Associate Editor of the IEEE SENSORS JOURNAL, from 2006 to 2016.

• • •